

# AD-A211 352 REPORT DOCUMENTATION PAGE

2

4a. SECURITY CLASSIFICATION AUTHORITY **SELECTED** **AUG 16 1989** **D**

2b. DECLASSIFICATION / DOWNGRADING SCHEDULE

1b. RESTRICTIVE MARKINGS

**FILE**

3. DISTRIBUTION / AVAILABILITY OF REPORT

Approved for public release and sale; its distribution is unlimited.

4. PERFORMING ORGANIZATION REPORT NUMBER(S)

Technical Report No. 67

5. MONITORING ORGANIZATION REPORT NUMBER(S)

6a. NAME OF PERFORMING ORGANIZATION  
Case Western Reserve University

6b. OFFICE SYMBOL  
(if applicable)

7a. NAME OF MONITORING ORGANIZATION  
ONR Chemistry Program

6c. ADDRESS (City, State, and ZIP Code)  
Cleveland, Ohio 44106

7b. ADDRESS (City, State, and ZIP Code)  
Arlington, Virginia 22217-5000

8a. NAME OF FUNDING / SPONSORING ORGANIZATION  
Office of Naval Research

8b. OFFICE SYMBOL  
(if applicable)

9. PROCUREMENT INSTRUMENT IDENTIFICATION NUMBER  
Contract N00014-83-K-0343

8c. ADDRESS (City, State, and ZIP Code)  
Arlington, Virginia 22217

10. SOURCE OF FUNDING NUMBERS

PROGRAM ELEMENT NO.	PROJECT NO.	TASK NO.	WORK UNIT ACCESSION NO.
	NR359-451		

11. TITLE (Include Security Classification)  
A Study of Bisulfate Adsorption on Pt(111) Single Crystal Electrodes using in-situ Fourier Transform Infrared Spectroscopy

12. PERSONAL AUTHOR(S)  
P.W. Faguy, N. Markovic, R.R. Adzic, C. Fierro and E. Yeager

13a. TYPE OF REPORT  
Technical Report

13b. TIME COVERED  
FROM 1988 TO 1989

14. DATE OF REPORT (Year, Month, Day)  
August 10, 1989

15. PAGE COUNT  
33

16. SUPPLEMENTARY NOTATION

COSATI CODES		
FIELD	GROUP	SUB-GROUP

18. SUBJECT TERMS (Continue on reverse if necessary and identify by block number)  
bisulfate adsorption; platinum single crystal electrodes; Fourier transform infrared

19. ABSTRACT (Continue on reverse if necessary and identify by block number)  
Subtractively normalized interfacial Fourier transform spectroscopy (SNIFTIRS) has yielded the first spectroscopic evidence that bisulfate anion adsorption is associated with the anomalous peaks seen in the cyclic voltammetry of Pt(111) in sulfuric acid. The infrared data indicates that the beginning of bisulfate anion adsorption coincides with onset of the anomalous peak region (+0.15 V vs SCE in 0.05 M H<sub>2</sub>SO<sub>4</sub>). The same IR spectra afford no evidence of sulfate anion adsorption on the Pt(111) single crystal electrode, over the potential range studied (-0.26 to +0.70 V vs SCE). Over this same potential region the adsorbed bisulfate absorption peak position showed a strong potential dependence. This increase in peak position with increasingly anodic potentials is rationalized using molecular orbital arguments.

89 8 14 095

20. DISTRIBUTION / AVAILABILITY OF ABSTRACT  
☒ UNCLASSIFIED/UNLIMITED ☐ SAME AS RPT ☐ DTIC USERS

21. ABSTRACT SECURITY CLASSIFICATION  
unclassified

22a. NAME OF RESPONSIBLE INDIVIDUAL  
Ernest Yeager, Professor of Chemistry

22b. TELEPHONE (Include Area Code) 22c. OFFICE SYMBOL  
(216)368-3626



OFFICE OF NAVAL RESEARCH

Research Contract N00014-83-K-0343

Technical Report No. 67

A STUDY OF BISULFATE ADSORPTION ON PT(111)  
SINGLE CRYSTAL ELECTRODES USING IN-SITU  
FOURIER TRANSFORM INFRARED SPECTROSCOPY

by

P. W. Faguy, N. Markovic, R. R. Adzic, C. Fierro and E. Yeager

Prepared for Publication

in the

Journal of Electroanalytical Chemistry  
and Interfacial Electrochemistry

Case Center for Electrochemical Sciences  
and the Department of Chemistry  
Case Western Reserve University  
Cleveland, Ohio 44106-2699

10 August 1989

Reproduction in whole or in part is permitted for  
any purpose of the United States Government.

This document has been approved for public release  
and sale; its distribution is unlimited.



Accession For	
NTIS CRA&I	<input checked="checked" type="checkbox"/>
DTIC TAB	<input type="checkbox"/>
Unannounced	<input type="checkbox"/>
Justification	
By	
Distribution /	
Availability Codes	
Dist	Avail and/or Special
A-1	



A STUDY OF BISULFATE ADSORPTION ON Pt(111) SINGLE CRYSTAL  
ELECTRODES USING *IN SITU* FOURIER TRANSFORM INFRARED SPECTROSCOPY

P. W. Faguy<sup>a</sup>, N. Markovic<sup>b</sup>, R. R. Adzic<sup>b</sup>, C. A. Fierro and E. B. Yeager  
Case Center for Electrochemical Sciences  
and the Department of Chemistry  
Case Western Reserve University  
Cleveland, Ohio 44106

ABSTRACT

Subtractively normalized interfacial Fourier transform spectroscopy (SNIFTIRS) has yielded the first spectroscopic evidence that bisulfate anion adsorption is associated with the anomalous peaks seen in the cyclic voltammetry of Pt(111) in sulfuric acid. The infrared data indicates that the beginning of bisulfate anion adsorption coincides with the onset of the anomalous peak region ( $\sim +0.15$  V vs SCE in 0.05 M H<sub>2</sub>SO<sub>4</sub>). The same IR spectra afford no evidence of sulfate anion adsorption on the Pt(111) single crystal electrode, over the potential range studied ( $-0.26$  to  $+0.70$  V vs SCE). Over this same potential region the adsorbed bisulfate absorption peak position showed a strong potential dependence. This increase in peak position with increasingly anodic potentials is rationalized using molecular orbital arguments.

INTRODUCTION

The origin of the reversible peaks appearing at potentials anodic of the hydrogen adsorption-desorption region on Pt(111) single crystal electrodes in acidic aqueous media is a topic of much interest and of some scientific controversy. These anomalous peaks were first discussed by Clavilier, who ascribed

---

<sup>a</sup>present address: Department of Chemistry, University of California, Davis CA 95616

<sup>b</sup>permanent address: Institute of Electrochemistry, ICTM, University of Belgrade, Belgrade, Yugoslavia.



these features to the adsorption and desorption of sub-monolayers of strongly bound hydrogen.<sup>1</sup> This hypothesis is based on the cyclic voltammetry for Pt(111) in 0.5 M H<sub>2</sub>SO<sub>4</sub>, 0.1 M HClO<sub>4</sub> and 0.1 M HCl. All the cyclic voltammetry showed unique peaks, but with quite different shapes and peak potentials for each different electrolyte.<sup>1</sup> Clavilier rationalized that the unique behavior for strongly bound hydrogen adsorption - desorption in each acidic electrolyte was caused by the existence of a unique adsorbate overlayer. The co-adsorbed anions are expected to have a large effect on the energetics of the strongly bound hydrogen state.

An alternative explanation is that in sulfuric acid electrolytes the anomalous peaks arise from sulfate or bisulfate anion adsorption and in perchlorate electrolytes the analogous peaks, at more positive potentials, stem from hydroxyl anion adsorption. This explanation originates from the analysis of literature data by Wagner and Ross for gas phase adsorption of hydrogen on platinum<sup>2</sup>. These workers concluded that an unreasonably large negative electro-sorption enthalpy would be required for adsorbed hydrogen to correspond to the very positive peaks formed on Pt(111) in perchloric acid and therefore ruled out this possibility. Instead for these peaks in perchloric acid they proposed the formation of an OH adsorbate. Al Jaaf-Golze *et al.*<sup>3</sup>, using cyclic voltammetry, and McIntyre *et al.*<sup>4</sup>, using a UV-vis electroreflectance technique arrived at the hypothesis that the anomalous peaks at +0.4 V vs NHE in sulfuric acid and +0.85 V in perchloric acid arise from anion adsorption and that hydrogen adsorption plays no significant role.

Using radiotracer and single crystal methodology, Krauskopf *et al.*<sup>5</sup> determined that the anomalous peak for Pt(111) in sulfuric acid correlate with the adsorption of sulfate and/or bisulfate anions. However, the maximum surface concentration of <sup>35</sup>S-containing species amounted to only ~7% of a monolayer and thus the electro-sorption valency necessary to account for the high charge



under the peak would be unrealistically large. They therefore proposed that "the anomalous charge is generated via a process that is activated by anion adsorption but is not directly derived from the anion adsorption."<sup>5</sup>

In recently published UHV - electrochemical work Wagner and Ross<sup>6</sup> support the interpretation that specifically adsorbed sulfate species are associated with the anomalous peaks. However, the extreme sensitivity of these voltammetric features to the Pt(111) surface structure has lead the Berkeley group to postulate that long-range structural effects of hydrogen-bonded aqueous clusters are the dominant factor in the anomalous behavior of Pt(111) electrodes in aqueous electrolytes.

The aim of this work is to advance the understanding of the role anion adsorption plays in such electrolytes. We report here the first combined use of single crystal flame annealing methodology and SNIFTIRS to probe the structure of the adsorbate layer on Pt(111) single crystal electrodes in a dilute sulfuric acid electrolyte.

#### EXPERIMENTAL

Fourier transform infrared measurements were made on an IBM Instruments IR-98A (Bruker 113v) Fourier transform spectrometer equipped with a liquid nitrogen cooled HgCdTe detector. The source, detector and interferometer chambers were kept under vacuum and were separated from the sample chamber via KBr windows. The sample chamber was left open to atmosphere and the instrument room was kept at  $21 \pm 0.5^\circ\text{C}$ . A commercially available (JAS Instruments) spectro-electrochemical cell was used for both the IR measurements and the cyclic voltammetry. The sampling optics consisted of an aluminum-KRS-5 wire grid polarizer, the cell, a refocusing 2" spherical mirror and two plane mirrors. The angle of incidence was  $65 \pm 2^\circ$  with beam divergence of  $12^\circ$  and a nominal beam diameter of 10 mm. The IR window was a  $\text{CaF}_2$  flat 2 mm thick and was polished to



1  $\mu\text{m}$  alumina before each measurement.

All the normalized relative reflectance  $-\Delta R/R$  spectra were obtained by co-adding 8192 scans at both reference and sample potentials, 128 scans at a time, switching between the sample potential and the reference potential a total of 128 times. A reference potential of  $-0.26\text{ V}$  vs. SCE was chosen, as  $\text{HSO}_4^-$  and  $\text{SO}_4^{2-}$  adsorption should be negligible at this potential. Spectra were taken at a resolution of 8 or  $16\text{ cm}^{-1}$ . The latter spectra were transformed with a zero filling factor of 4 and no smoothing while the former were transformed with ZFF-2 and smoothed with a Savitsky-Golay algorithm of order 3. No discernable differences were found between the two data processing schemes.

The methodology of electrode preparation including polishing, cleaning, flame annealing, cooling in  $\text{H}_2$ , quenching with water and formation of a meniscus-type electrochemical cell is detailed in reference 7. The single crystal Pt(111) electrode (Metal Crystal Ltd; Cambridge, England) used for the spectroscopic measurement, was 8 mm in diameter by 4 mm thick and was oriented and cut to better than  $1^\circ$ . The single crystal Pt(111) electrode (Metal Crystal Ltd; Cambridge, England) used for the comparison cyclic voltammetry was 6.35 mm in diameter by 6.35 mm thick and was oriented and cut to better than  $1^\circ$ . Water distilled after reverse osmosis was used to make the sulfuric acid (Baker Ultrex) solutions.

The larger single crystal electrode, after preparation, was mounted in a specially constructed Teflon holder. The right cylinder electrode was pressed into the inside  $2^\circ$  taper of the holder which also allowed the single crystal polished face to align parallel to the  $\text{CaF}_2$  window. The polished electrode face and approximately 0.5 mm of the cylinder edge were exposed to the electrolyte. Before pressing the single crystal electrode fully into the Teflon holder cyclic voltammetry was recorded to confirm that the platinum surface



corresponded to Pt(111) and was of reasonable crystallographic quality. Figure 1 indicates the cell - electrode configurations for cyclic voltammetry and for SNIFTIRS. After obtaining acceptable cyclic voltammetry, the electrode was pressed against the  $\text{CaF}_2$  window under potential control. The cell was then disconnected, transferred to the FTIR spectrometer and potential control re-established. Cyclic voltammetry was also performed on the 6.35 mm Pt(111) electrode using an optimized electrochemical cell.<sup>7</sup>

## RESULTS AND DISCUSSION

In the course of this work it was found that the procedures involved in forming a thin layer cell between the Pt(111) electrode surface and the  $\text{CaF}_2$  window were crucial to the success of the spectroscopic experiment. If the electrode was ever exposed to the atmosphere, following the quenching step, or if the meniscus was broken and remade, the subsequent spectra did not show the expected features. The adsorption of organic impurities over the entire potential range (including the reference potential) was probably the cause of this effect.

Using the electrode - cell orientation in Figure 1a the cyclic voltammogram shown in Figure 2 was obtained. The anomalous peaks at  $\sim 0.2$  V vs SCE are observed with the first anodic and cathodic sweeps as well as in subsequent cycles. These peaks are essentially reversible. Cyclic voltammetry of Pt(111) in 0.05 M  $\text{H}_2\text{SO}_4$  obtained using a traditional electrochemical cell is shown in Figure 3. This curve represents cyclic voltammetry for flame-annealed Pt single crystals measured under optimum conditions, while Figure 2 shows the same CV taken in a cell designed for spectroelectrochemical measurements. The two curves demonstrate that both electrodes have well ordered (111) oriented surfaces. In comparing the two curves, the CV taken in the spectroelectrochemical cell shows an asymmetry of cathodic current, a more sloped onset of hydrogen



adsorption and a reduction in the size of the sharp anomalous peak. The asymmetric cathodic current is due to some oxygen in the electrolyte and the other differences are probably due to traces of organic impurities. The charges under the anomalous peak, from Figure 2,  $82 \mu\text{C}/\text{cm}^2$ , and from Figure 3,  $80 \mu\text{C}/\text{cm}^2$  agree with values already present in the literature.<sup>7</sup>

Table 1 lists the vibrational bands for the bisulfate and sulfate anions. The peak positions for the  $\text{SO}_4^{2-}$  anion are taken from IR data for aqueous solutions.<sup>8</sup> The  $\text{C}_{3v}$  symmetry group for the  $\text{HSO}_4^-$  anion is arrived at by treating the hydroxyl moiety as a point mass<sup>9</sup>, and the peak positions are representative of  $\text{HSO}_4^-$  in aqueous solution and in crystal hydrates.<sup>9,10</sup> There are five possible bands which fall in the observable region of the *in situ* experiment, and of these only three can be seen when a  $\text{CaF}_2$  window is used. These bands are the symmetric stretch of bisulfate,  $\nu_s(\text{HSO}_4^-)$ , at  $\sim 1050 \text{ cm}^{-1}$ , the double degenerate asymmetric stretch of bisulfate,  $\nu_{as}(\text{HSO}_4^-)$  and the triply degenerate stretch of sulfate,  $\nu_s(\text{SO}_4^{2-})$ . The symmetric sulfate stretch and the S-OH stretch of bisulfate occur below the lower wavenumber cutoff of the  $\text{CaF}_2$  window.

On polycrystalline Pt electrodes other groups<sup>12-15</sup> have identified two bands in the *in situ* infrared reflectance spectra. Russell *et al.*<sup>12</sup>, using electrochemically modulated infrared spectroscopy EMIRS, attribute the  $1200 - 1250 \text{ cm}^{-1}$  band to the  $\nu_s(\text{HSO}_4^-)$  mode and the lower frequency peak,  $\sim 1100 \text{ cm}^{-1}$ , to the  $\nu_{as}(\text{HSO}_4^-)$  vibration, as does Scharifker *et al.*<sup>13</sup> using polarization modulation FTIRRS. For the same system and for similar data, researchers at IBM San Jose<sup>14,15</sup>, using SNIFTIRS, concur with the assignment of the  $1200 - 1250 \text{ cm}^{-1}$  band to the bisulfate asymmetric stretch but assign the lower frequency peak to the  $\nu_s(\text{SO}_4^{2-})$  vibrational mode.

Figures 3 and 4 shows the SNIFTIR spectra obtained in our laboratory for a Pt(111) single crystal electrode in  $0.05 \text{ M H}_2\text{SO}_4$  over the potential region from



hydrogen adsorption to just before the onset of Pt oxidation. It should be noted that spectra shown could be obtained in any order and in a very reversible manner. Once the clean Pt(111) electrode had been introduced into the thin layer cell, there was no evidence of contamination over three days of data taking. The difference in peak positions for replicate runs was less than  $4\text{ cm}^{-1}$ , which is well within the actual experimental resolution of  $8\text{ cm}^{-1}$ .

Only one positive going band is found in the spectral region associated with stretching modes of the  $\text{HSO}_4^-$  and  $\text{SO}_4^{2-}$  anions. This indicates that the spectra arise from a potential dependent adsorption of a single species. At potentials near the onset of the anomalous CV peaks the SNIFTIRS peak is broad and weak with a peak position of approximately  $1200\text{ cm}^{-1}$ . As the potential is moved anodic the band becomes more intense and the peak position shifts substantially. At  $0.7\text{ V}$  the peak position is almost  $1300\text{ cm}^{-1}$ . There is also some evidence from the change in line shape as the potential is increased that there may be several modes involved. The deconvolution of bands in the  $1200 - 1280\text{ cm}^{-1}$  envelope necessary to analyze this effect is beyond the scope of this work.

The absorption band between  $1200 - 1280\text{ cm}^{-1}$  can be assigned to the  $\nu_{\text{as}}$  mode of the  $\text{HSO}_4^-$  ion based on the bulk solution phase values for the same transition. This peak can also be ascribed to a specifically adsorbed species based on the potential dependence of the peak position. There are three possible orientations on the electrode surface depending on the number of Pt - O interactions. These orientations are schematically shown in Figure 6. This high frequency band can be assigned to the same processes in both the Pt(111) and the polycrystalline Pt data<sup>12-15</sup>. The effect of the surface on the vibrational bands relative to the same modes for the solution phase species is twofold: the force constant associated with each mode can be changed due to



bonding interactions with the electrode surface and the symmetry of the complex is necessarily lowered.

This means the IR peaks due to surface species may be shifted and broadened relative to those for solution phase species. Also these two effects will have different electrochemical potential dependencies. A distribution of bands could be a function of surface crystallographic orientation as well as of electrode potential. Since the force constant associated with a given band can also be a function of potential the assignment of a series of potential dependent absorptions to either an orientational change or a change in bonding interaction with the surface is tentative. Based on coverage and molecular orbital arguments made further on in this paper we assign the asymmetric  $(\text{SO})_3$  stretch of the trigonally coordinated bisulfate ion (Figure 6c) as the predominant component of the  $1200 - 1280 \text{ cm}^{-1}$  band.

The lack of any spectral features around  $1100 \text{ cm}^{-1}$  (Figure 4) for the single crystal experiments, relative to that seen in the  $1200 - 1300 \text{ cm}^{-1}$  region (Figure 3), is the most significant difference between the Pt(111) data and the polycrystalline data.<sup>12-15</sup> For the Pt(111) SNIFTIRS data, the intensity of any band near  $1100 \text{ cm}^{-1}$  is either zero or orders of magnitude less than the transition at  $1200 - 1280 \text{ cm}^{-1}$  while the polycrystalline experiments shows comparable peak heights in both regions.<sup>12-15</sup> Although the position of this low frequency absorption is identical to the solution phase sulfate mode, there is evidence<sup>14</sup> that it is an adsorbed species. Either the symmetric bisulfate stretch or the triply degenerate sulfate stretch can be assigned to this band in the  $1050 - 1100 \text{ cm}^{-1}$  region.

In  $0.05 \text{ M H}_2\text{SO}_4$ , using  $K_2 = 1.02 \times 10^{-2}$  for the second dissociation constant, there are 5 - 6 bisulfate anions for every sulfate anion present in the bulk solution. Based on this concentration argument and the bulk phase absorption value ( $\sim 1050 \text{ cm}^{-1}$ ), the low frequency band observed in the



polycrystalline case could be assigned to the  $\nu_s(\text{HSO}_4^-)$  mode. If the  $\sim 1100\text{ cm}^{-1}$  peak is due to a bisulfate absorption then there must be some restriction of this transition in the Pt(111) case relative to the polycrystalline case, as the species responsible for such an absorption, bisulfate, is present on the electrode in both cases, yet only peaks in the polycrystalline IR spectra are seen.

A simpler explanation is that sulfate, adsorbing at surface sites present on the polycrystalline electrode but not on the Pt(111) electrode, is responsible for the peak seen in the  $1050 - 1150\text{ cm}^{-1}$  region of the *in situ* IR reflectance spectra obtained on polycrystalline Pt electrodes. A firm conclusion on whether this absorption is due to surface or diffuse-layer species or whether it is due to sulfate or bisulfate ions awaits further experiments.

The potential dependence of the bisulfate peak position is shown in Figure 7. The slope of a best fit line through the points gives a value of  $108\text{ cm}^{-1}\text{V}^{-1}$ . For the polycrystalline case the potential dependency of the bisulfate peak<sup>15</sup> is  $100\text{ cm}^{-1}\text{V}^{-1}$ . These two slopes are similar enough to consider the same mechanism operable in both cases, as would be expected for the same adsorbate - surface site interaction occurring on both electrodes.

A positive slope of  $108\text{ cm}^{-1}\text{V}^{-1}$  is a large potential dependent shift. In comparison, carbon monoxide on single crystal Pt(111) surfaces in sulfuric acid shows a  $+30\text{ cm}^{-1}\text{V}^{-1}$  slope.<sup>16</sup> The shift of CO stretching frequency on Pt with increasing anodic potential has been explained by Ray and Anderson<sup>17</sup> using the atom superposition electron delocalization molecular orbital (ASED-MO) technique. They have shown that the back bonding interaction between the Pt d band and the C-O  $\pi^*$  orbital is weakened as the Pt valence band moves towards higher binding energy (i.e.; is shifted anodic of the pzc) and thus the C-O



bond strengthens and the vibrational frequency increases.

A similar explanation may be valid in the case of bisulfate adsorption on Pt(111) electrode surfaces. Using the ASED-MO approach, the molecular orbitals for  $\text{HSO}_4^-$  were constructed with bond lengths and bond angles from the literature<sup>18</sup> and atomic orbital parameters used by Anderson in other ASED-MO calculations.<sup>19</sup> The highest occupied molecular orbital (HOMO) is non-bonding oxygen lone pair orbital delocalized through the oxygen atoms with no sulfur contribution. These are the donating orbitals responsible for the forward  $\sigma$  bonding with empty Pt states.

The lowest unoccupied molecular orbitals (LUMOs) are two different molecular orbitals of similar energy; a  $\pi^*$  bisulfate orbital present on the O-S-O fragment *cis*-coplanar to the O-H bond and  $\sigma^*$  MO involving the two S-O fragments not co-planar with the O-H bond. These antibonding orbitals, shown in Figure 8, could accept charge back-donated from the Pt 5d band. The geometric contribution from the Pt orbitals involved has not been treated at all here, as the metal bonding orbitals are expected to be oriented out of the Pt surface plane and thus the main symmetry concerns rest with the bisulfate molecular orbitals.

The  $\sigma$  bonding interaction between the bisulfate HOMO and the empty metal 5d band in Pt -  $\text{HSO}_4^-$  should show a much slower dependence on potential than the back donation from Pt(111) valence band to the empty bisulfate LUMOs, in direct analogy to the Pt - CO case.<sup>17</sup> Quantitatively the effect should even be larger for the Pt -  $\text{HSO}_4^-$  than for the Pt - CO case because  $\sigma$  back donation is intrinsically stronger than  $\pi$  back donation. This trend is in agreement with value of  $100 \text{ cm}^{-1}\text{V}^{-1}$  for Pt -  $\text{HSO}_4^-$  relative to  $30 \text{ cm}^{-1}\text{V}^{-1}$  for Pt - CO. Efforts to arrive at a more complete molecular orbital picture, including both the sulfate dianion and the Pt surface in a quantitative way are being undertaken.

The orientation of the bisulfate distorted tetrahedron on the Pt(111)



surface should involve the greatest possible overlap between the HOMO of the anion and the available empty metal states. As the lone pair orbitals lie perpendicular to the S-O bond there could be substantial overlap between these p orbitals and the metal conduction band through either 3-fold, 2-fold or 1 fold sites. Table 2 lists some symmetry and geometry related parameters for the three different orientations of the bisulfate anion on the Pt(111) surface. As shown in column 3 of Table 2, all three possible orientations could provide orbital overlap.

In order for an infrared transition to occur the vibrational mode and the electric dipole operator must belong to the same irreducible representation. For anisotropic species this imposes a set of symmetry imposed orientational selection rules in addition to the usual quantum mechanical ones. The z axis of the molecule coincides with the S-OH bond and the xy plane is parallel to the plane containing the three unprotonated oxygens. Because of the symmetry there is no unique definition of the x and y axes. In Table 2 the 7th column lists the projection of a unit dipole vector for the particular mode on the surface normal for the three different adsorption geometries.

While a mode may be allowed from quantum mechanical and symmetry selection rules its intensity depends on the physical optics of reflection from a metal surface, i.e.; the surface selection rule. The projection of the allowed dipole vector on the surface normal (the 7th column of Table 2) is a crude measure of the combined effects of symmetry and surface selection rules.

From these symmetry and physical optics considerations, ignoring vibronic coupling, hydrogen bonding or any effects due to the applied electric field and the presence of the double layer, the following points can be made. For a 3-fold adsorption geometry, possessing  $C_{3v}$  symmetry, only the  $m_s$  mode would be observed, the asymmetric stretch would be polarized in the xy plane and would



have no intensity. Both the 2-fold and 1-fold orientations belong to the  $C_s$  point group. As the symmetry is lowered the effect is to split the degenerate  $\nu_{as}$  mode from the E irreducible representation in the  $C_{3v}$  point group to the  $A'$  and  $A''$  representations in the  $C_s$  point group. This should be seen as a splitting of the higher frequency mode. As the dipole overlap column of Table 2 shows the overlap with the surface normal is non-zero for all modes in both the 2-fold and 1-fold orientations.

The expected hypothetical spectra for a 3-fold adsorption site would contain only the  $\sim 1050\text{ cm}^{-1}$  while the same IR data for the 2-fold and 1-fold sites would show a splitting of the  $\sim 1200\text{ cm}^{-1}$  peak and also the symmetric lower frequency stretch.

The Pt(111) and the polycrystalline results do not support the above simple predictions probably because the effect of the metal surface, the local solution environment and the applied potential have a large effect on the spectra. A thorough treatment of these processes is beyond the scope of this work and the present level of theory concerning infrared transitions for molecules adsorbed at the electrode-electrolyte interface. Some mention may be made of vibrational electronic coupling effects which have been invoked to explain several IRRAS experimental results<sup>22</sup> where the surface selection rule appeared to be broken.

The electric field at the electrode - electrolyte interface is on the order of  $10^7\text{ V/cm}$ , this field is large enough to induce a Stark effect.<sup>23</sup> The removal of the rotational ground state degeneracy would cause absorptions not normally IR active to become active and also to effect the intensity of already allowed transitions. Bewick's group<sup>12</sup> postulate this as a mechanism by which the  $\text{HSO}_4^-$   $\nu_{as}$  mode can be assigned to the high frequency peak. The electrochemical Stark effect is a vibronic coupling caused by the presence of a large



electric field arising from the applied potential across the electrode / electrolyte interface.

Another quantity often obtained from the FTIRRA spectra electrochemical potential relationship is the dependence of integrated band intensity on potential. If the dielectric constants of the electrolyte and the electrode vary negligibly over the potential range, and the oscillator strengths of the modes involved in the absorption are similar for each potential measured, then the integrated band intensity can be directly related to the surface coverage. In order to account for the fact that these are reflectance spectra rather than transmission spectra, it is necessary to apply the simplified form of the Fresnel equations which holds for layer thicknesses much less than the wavelength of the reflected light.<sup>24</sup> The quantity related linearly to surface coverage is the ratio of the integrated band intensity to the difference of the squares of the integration limits. In Figure 9 the 'corrected' band intensity is plotted against Pt electrode potential. The effect of correcting the integrated band intensity is minor as the integration limits used were quite similar for all cases and the reported numbers are normalized. Due to the relatively poor signal-to-noise ratio in the  $-\Delta R/R$  spectra, the uncertainty in the ordinate values is on the order of 15%. Because of this large uncertainty it is not clear whether the integrated intensity shows any Stark effect electric field dependency.

If the charge under the anomalous oxidation peak in the CV of Pt(111) in 0.05 M sulfuric acid is due primarily to the adsorption of bisulfate ions then there should be some correspondence between the curve seen in Figure 8 and the plot of charge versus potential for the anomalous oxidation peak. The charge as a function of potential was obtained from the curve shown in Figure 2 after correcting for double layer and hydrogen desorption contribution. In the literature there are data relating surface coverage of <sup>35</sup>S-containing species



to the electrode potential for the same system.<sup>5</sup> Figure 10 shows the normalized plot of these three quantities, charge (from Figure 2), corrected band intensity and surface coverage of <sup>35</sup>S-containing species versus potential.

All three curves shown in Figure 10 have the onset of positive slope within 50 mV of each other just positive of 0.0 V vs SCE. Also there is some agreement among the shapes of the curve over the potential region where the anomalous peaks occur. These observations support the hypothesis that the anomalous peaks are associated with the adsorption of bisulfate anions, however this data yields little information to address the problem of such a high charge associated with the peak and with an abnormally high charge to coverage ratio as obtained by Krauskopf *et al.*<sup>6</sup>

In analysis of this peak one has to consider the three-fold geometry of the tetrahedral structure of the bisulfate ions and the trigonal symmetry of the atomic arrangement on a (111) surface. This has been stressed by Angerstein-Kozłowska and co-workers who found a full discharge of bisulfate ions on Au(111) electrodes.<sup>25,26</sup> After correcting for the double layer charging, they arrived at an excess charge of 47  $\mu\text{C}/\text{cm}^2$  for 0.1 M  $\text{H}_2\text{SO}_4$  on Au(111) at  $E_{\text{peak}} \approx 0.7$  V vs RHE. The CV's in Figures 2 and 3 were corrected for residual double layer current and then the charge under the corrected peak was calculated. The corrected charge under the peak in Figure 2 (the spectroelectrochemical cell), 54  $\mu\text{C}/\text{cm}^2$ , agrees well with the value calculated from the CV shown in Figure 3, 60  $\mu\text{C}/\text{cm}^2$ . These values are comparable to the excess charge measured on Au(111) electrodes in, however, a wider potential region.<sup>25</sup>

The less positive peak potential and more localized process found for the Pt(111) voltammetry over that for the Au(111) CV can certainly be related to the higher adsorption reactivity generally found with platinum. The interatomic distance for vicinal Pt atoms on a Pt(111) plane is 2.77 Å, which could



accommodate a  $\text{HSO}_4^-$  anion with a partial hydration sheath. In the case of Pt(111), as is the case for Au(111), bisulfate adsorption causes an exceptional shift of the oxide formation reaction to very anodic potentials. This is probably due to the effective blocking of (111) sites by tetrahedral ions.

SNIFTIRS data were taken at potentials as anodic as +0.9 V, a potential at which the toe of the Pt oxide formation peak is seen. In this region hydroxyl ion adsorption begins<sup>3,4</sup> and the adsorbed bisulfate anion is desorbed. Figure 11 demonstrates the large change that takes place in the nature of the sulfuric acid anions at the electrode surface. At 0.7 V the major bisulfate band is still present at  $1279\text{ cm}^{-1}$ , perhaps with a shoulder appearing at  $1253\text{ cm}^{-1}$  as is shown in figure 11, curve a. The peak position of  $1279\text{ cm}^{-1}$  for the bisulfate asymmetric  $\text{SO}_3$  stretching mode is still consistent with the trigonal coordinated adsorbate proposed earlier. When the sample potential is raised to 0.9 V the spectrum is changed drastically. According to the quasi-linear trend of peak positions with potential (see figure 6), the adsorbed bisulfate peak should have appeared at  $\sim 1310\text{ cm}^{-1}$ , but instead a broad band appears at  $1194\text{ cm}^{-1}$  with a weaker, unresolved broad band at  $1112\text{ cm}^{-1}$ . This spectrum is shown in figure 11, curve b.

The spectra reported by the IBM San Jose group<sup>14,15</sup> for a polycrystalline Pt electrode in 0.05 M  $\text{H}_2\text{SO}_4$  at +0.75 V vs RHE shows peaks at 1234 and  $1119\text{ cm}^{-1}$ . The  $1234\text{ cm}^{-1}$  peak for polycrystalline Pt is still demonstrating the positive going peak shift with potential while the  $1194\text{ cm}^{-1}$  peak for Pt(111) shows a radical departure from such a trend. The  $\sim 1120\text{ cm}^{-1}$  peak for polycrystalline Pt occurs at lower potentials with a constant band intensity above +0.45 V vs RHE while the  $1112\text{ cm}^{-1}$  band for Pt(111) at +0.9 V vs SCE has no analogs at more cathodic potentials. The IBM researchers assign the higher frequency band to adsorbed  $\text{HSO}_4^-$  and the lower frequency one to adsorbed  $\text{SO}_4^{2-}$ .

A similar assignment for the +0.9 V vs SCE Pt(111) FTIRRA spectra is not



possible. The position of the peaks in figure 11, curve b cannot be due to a potential dependent adsorbed bisulfate species on the Pt(111); there is no mechanism for such a large change in the S-O force constant. Invoking  $\text{SO}_4^{2-}$  adsorption would require some rationale for there being no sulfate bands present at more cathodic potentials. The abrupt change in the IR spectrum occurs with the onset of Pt-oxide formation (figure 11). The important factors affecting the spectra are the increase in adsorbed hydroxyl ion concentration and the decrease in adsorbed bisulfate ion concentration. The spectral features due to remaining  $\text{HSO}_4^-$  on the surface will be greatly modified by the neighbouring  $\text{OH}^-$  species; not only will the intensity of the bisulfate peaks change but also the position will shift. Perhaps more importantly, the charge neutrality condition at the interface will change. The relative magnitudes of metal charge density, adsorbate charge density and diffuse layer charge density will be quite different from those charge densities before hydroxyl adsorption or, equivalently, Pt oxide formation.

When the sample and the reference spectra demonstrate very different diffuse layer anion concentrations, a condition that can occur either when the nature of the adsorbate changes or when the potential difference is great, then diffuse layer spectral features will become predominate. Considering these factors the two broad peaks seen in Figure 11, curve b are probably due to solution phase species present in the double layer with any contribution from adsorbed species buried in the broad shoulders. The position of the bands, as well as their breadth, is in agreement with a tentative assignment of the  $1194\text{ cm}^{-1}$  band to the doubly degenerate stretching mode of  $\text{HSO}_4^-$  and the  $1112\text{ cm}^{-1}$  band to the  $\text{T}_2$  stretching mode of  $\text{SO}_4^{2-}$ . In order to test these assignments it would be productive, in future work, to include species in the electrolyte which adsorb much more strongly (e.g.; CO) which would preclude sulfate /



bisulfate specific adsorption<sup>14</sup> and alternatively to include ionic species in the electrolyte which adsorb much more weakly, (e.g.;  $\text{ClO}_4^-$  salts) which would eliminate any bulk phase sulfate / bisulfate contribution due to diffusion.<sup>27</sup>

## CONCLUSIONS

*In situ* Fourier transform infrared spectroscopy has yielded evidence that from 0.05 M  $\text{H}_2\text{SO}_4$  solution  $\text{HSO}_4^-$  is the predominantly adsorbed species at potentials cathodic of any Pt oxide formation. The onset of the SNIFTIRS peak correlates with the anomalous CV peaks. Based on coverage / charge arguments and on a simple MO picture we propose that the major bisulfate orientation is on a three-fold site, each of the unprotonated oxygens interacting with a Pt atom. Investigation of other vibrational modes, at lower frequencies than those accessible with the  $\text{CaF}_2$  window, would be helpful in definitive determination of this orientation. The large potential dependency of the bisulfate absorption peak position is qualitatively explained in terms of back-bonding electrode - adsorbate interactions.

The appearance of only one band in the Pt(111) case contrasts with the appearance of two absorptions in the polycrystalline case. The high frequency band in both cases has been ascribed to the asymmetric bisulfate SO stretch.<sup>12-15</sup> While the low frequency band appears to be due to the  $\nu_s(\text{SO}_4^{2-})$  normal mode in the polycrystalline case and is not observed in the Pt(111) spectra.

A possible explanation of the large charge measured under the CV peak at  $\sim 0.1$  V vs SCE is the sizable discharge of a monolayer of 3-fold coordinated bisulfate. However this conclusion is not supported by the Pt(111) -  $^{35}\text{S}$  radio-tracer studies<sup>5</sup>, and warrants further study.



#### ACKNOWLEDGMENTS

The authors wish to thank Frank Feddrix for performing some of the cyclic voltammetry and Intae Bae for many helpful discussions. The support of this research by the U.S. Office of Naval Research is gratefully acknowledged.



## References

- 1) J. Clavilier, *J. Electroanal. Chem.*, 107 (1980) 211.
- 2) F.T. Wagner and P.N. Ross, *J. Electroanal. Chem.*, 150 (1983) 141.
- 3) K. Al Jaaf-Golze, D.M. Kolb and D. Scherson, *J. Electroanal. Chem.*, 200 (1986) 353.
- 4) J.D.E. McIntyre, W.F. Peck Jr., J. Lipkowski and B. Love, Abstract No. 520 presented at the Spring Meeting of the Electrochemical Society, Atlanta, GA 1988.
- 5) E.K. Krauskopf, L.M. Rice and A. Wieckowski, *J. Electroanal. Chem.*, 244 (1988) 347.
- 6) F.T. Wagner and P.N. Ross, Jr., *J. Electroanal. Chem.*, 250 (1988) 301.
- 7) N. Markovic, M. Hanson, G. McDougall and E. Yeager, *J. Electroanal. Chem.*, 214 (1986) 555.
- 8) P.A. Griguere and R. Savoie, *Can. J. Chem.*, 38 (1960) 2467.
- 9) B.S. Dawson, D.E. Irish and G.E. Toogood, *J. Phys. Chem.*, 90 (1986) 334.
- 10) J.H.R. Clarke, L.A. Woodward, *Trans. Faraday Soc.*, 57 (1961) 1286.
- 11) K. Nakamoto "Infrared Spectra of Inorganic and Coordination Compounds" John Wiley & Sons: New York, 1963, p111-112.
- 12) J.W. Russell, M. Razaq and A. Bewick, Abstract No. 332 presented at the Spring Meeting of the Electrochemical Society, Atlanta, GA 1988.
- 13) B.R. Scharifker, K. Chandrasekaran, M.E. Gamboa-Aldeco, P. Zelenay and J.O'M. Bockris, *Electrochim. Acta*, 33 (1988) 159.
- 14) K. Kunimatsu, M.G. Samant, H. Seki and M.R. Philpott, *J. Electroanal. Chem.*, 243 (1988) 203.
- 15) K. Kunimatsu, M.G. Samant, H. Seki and M.R. Philpott, Abstract No. 105 presented at the 39th Meeting of the International Society of Electrochemistry, Glasgow, Scotland, 1988.
- 16) N. Furuya, S. Motoo and K. Kunimatsu, *J. Electroanal. Chem.*, 239 (1988) 347.
- 17) N.K. Ray and A.B. Anderson, *J. Phys. Chem.*, 86 (1982) 4851.
- 18) Z. Mielke and H. Ratajczak, *J. Mol. Structure*, 18 (1973) 493.
- 19) A.B. Anderson and N.C. Debnath, *J. Phys. Chem.*, 87 (1983) 1938.
- 20) N.M. Markovic, N.S. Marinkovic and R.R. Adzic, *J. Electroanal. Chem.*, 241 (1988) 309.



- 21) Anderson, A.B. *Surf. Sci.*, 183 (1987) 438.
- 22) K. Ashley and S. Pons. *Chem. Rev.*, 88 (1988) 673.
- 23) C. Korzeniewski, R.B. Shirts and S. Pons, *J. Chem.* 89 (1985) 2297.
- 24) J.D.E. McIntyre in *Advances in Electrochemistry and Electrochemical Engineering*, Vol. 9 P. Delahay and C. Tobias Eds., Interscience, New York, 1973 p. 61.
- 25) H. Angerstein-Kozłowska, B. Conway, A. Hamelin and L. Stoicoviciu, *Electrochim. Acta* 31 (1986) 1051.
- 26) H. Angerstein-Kozłowska, B. Conway, A. Hamelin and L. Stoicoviciu, *J. Electroanal. Chem.*, 228 (1987) 429.
- 27) D.S. Corrigan and M.J. Weaver, *J. Electroanal. Chem.*, 239 (1988) 55.



Table 1. Vibrational frequencies of bisulfate and sulfate anions.

NORMAL MODE	DESCRIPTION <sup>a</sup>	POSITION <sup>b</sup> (cm <sup>-1</sup> )
<b>HSO<sub>4</sub><sup>-</sup> (C<sub>3v</sub> symmetry)</b>		
$\nu_1(A_1)$	symmetric (SO <sub>3</sub> ) stretch	~1050
$\nu_2(A_1)$	symmetric S-OH stretch	890 - 900
$\nu_3(A_1)$	symmetric (SO <sub>3</sub> ) deformation	590 - 600
$\nu_4(E)$	asymmetric (SO) <sub>3</sub> stretch	~1200
$\nu_5(E)$	asymmetric (SO <sub>3</sub> ) deformation	400 - 420
$\nu_6(E)$	asymmetric (SO <sub>3</sub> ) rock	590 - 600
<b>SO<sub>4</sub><sup>2-</sup> (T<sub>d</sub> symmetry)</b>		
$\nu_1(A_1)$	symmetric (SO) stretch	~980
$\nu_2(E)$	asymmetric (OSO) deformation	~450
$\nu_3(T_2)$	triply degenerate (SO) stretch	1090 - 1210
$\nu_4(T_2)$	triply degenerate (OSO) deformation	~640

<sup>a</sup> Notation is consistent with that used in references 10 and 11.

<sup>b</sup> Peak locations from references 8-10.



Table 2. Effect of coordination on bonding overlap and symmetry for possible orientations of  $\text{HSO}_4^-$  on  $\text{Pt}(111)$ .

Figure	Number of Coord. Sites	Geometric Overlap ( $\cos \alpha$ ) <sup>a</sup>	Group Symmetry Representation	IR Active Mode <sup>c</sup>	Dipole Moment Vector	Dipole Overlap ( $\cos \beta$ ) <sup>b</sup>
free ion	0	-	$C_{3v}$	$A_1 (\nu_1)$ $E (\nu_4)$	$D_z$ $D_x, D_y$	- -
6a	3	3 x 0.33	$C_{3v}$	$A_1$ $E$	$D_z$ $D_x, D_y$	1.0 0.0
6b	2	2 x 0.58	$C_s$	$2A'$ $A''$	$D_z$ $D_x, D_y$	0.58 0.81
6c	1	1 x 1.0	$C_s$	$2A'$ $A''$	$D_z$ $D_x, D_y$	0.33 0.94

<sup>a</sup>  $\alpha$  is the angle between the surface normal and the S-O bond.

<sup>b</sup>  $\beta$  is the angle between the surface normal and the dipole moment vector.

<sup>c</sup> See Table 1 for description and text for details.



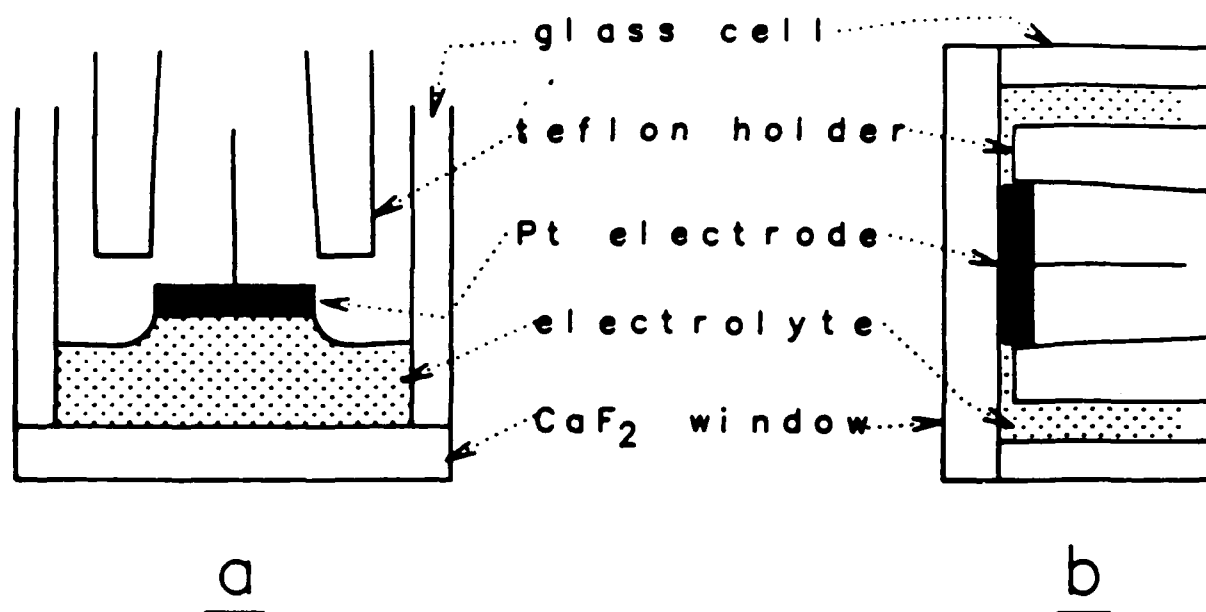
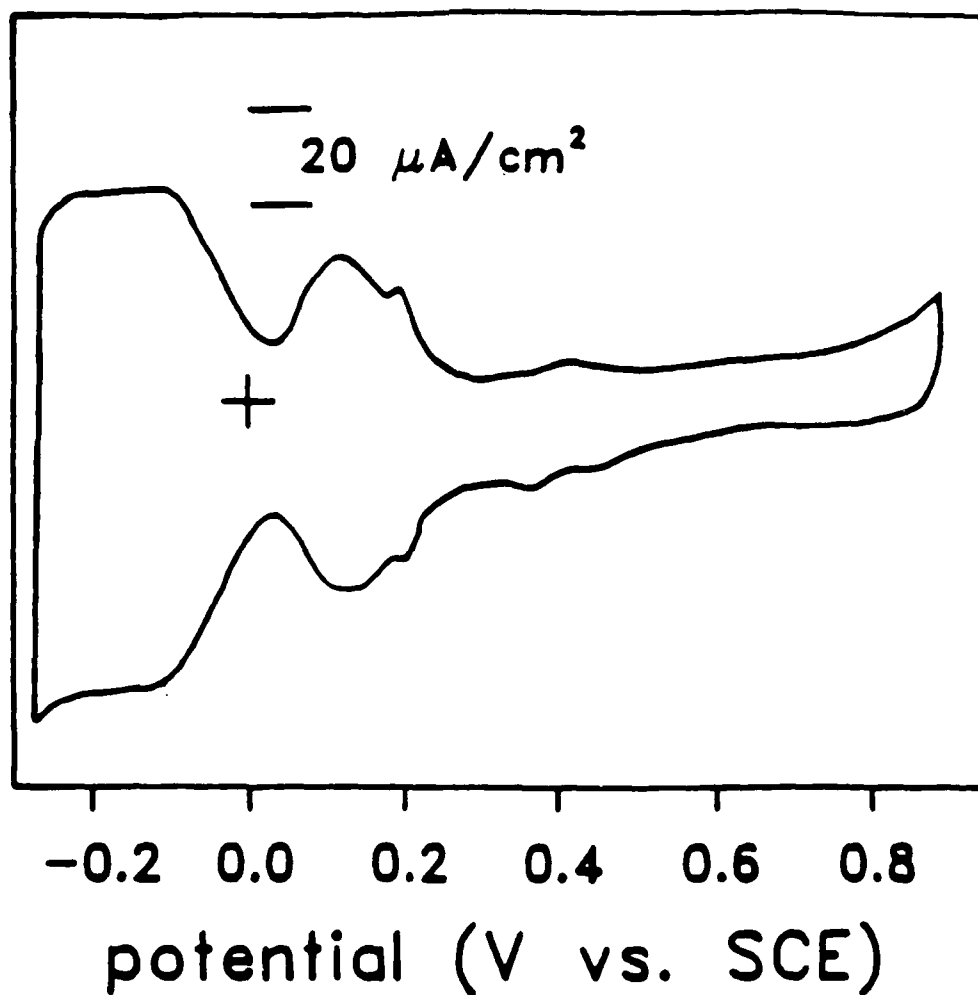


Figure 1. Schematic diagram of spectroelectrochemical cell as used for a) cyclic voltammetry and b) IR spectroscopy.





**Figure 2.** Cyclic voltammogram for flame-annealed Pt(111) single crystal electrode in 0.05 M  $\text{H}_2\text{SO}_4$  electrolyte using meniscus method in a cell subsequently used for spectroelectrochemical measurements as shown in Fig. 1a. Sweep rate was 50 mV/s.



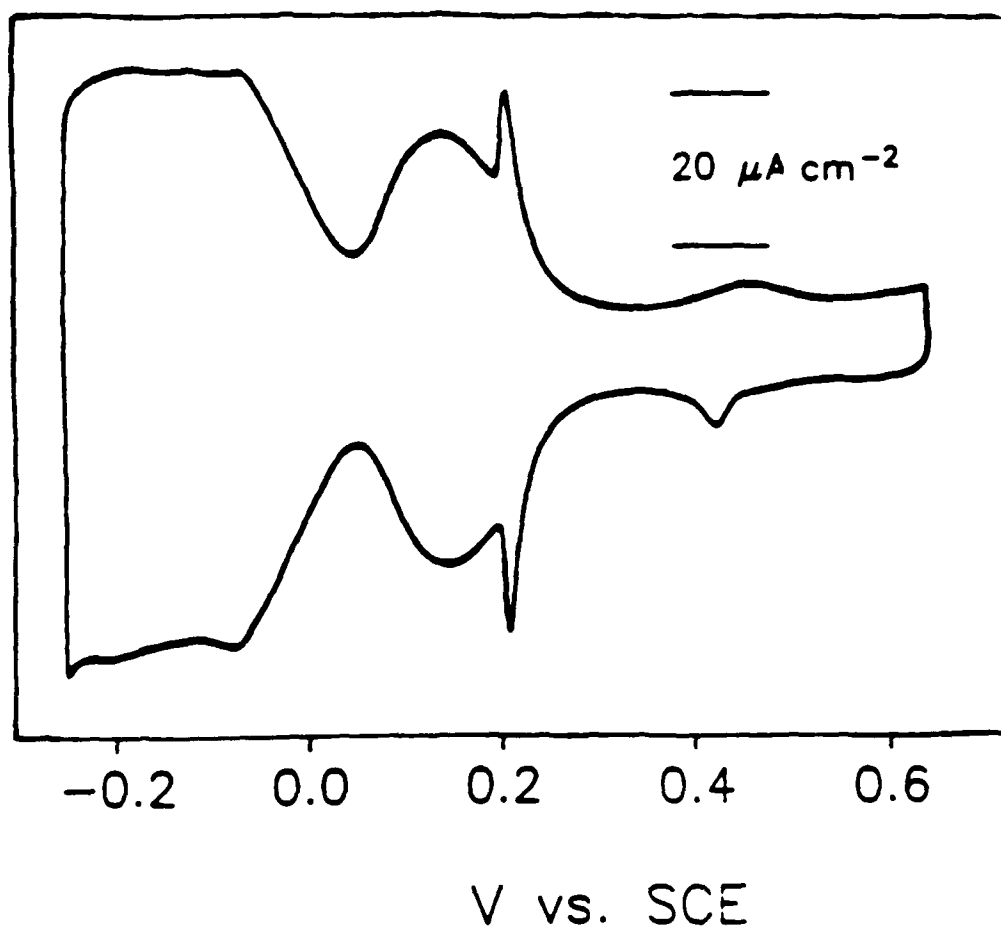


**Figure 3.** Cyclic voltammogram for 6.5 mm flame-annealed Pt(111) single crystal electrode in 0.05 M  $\text{H}_2\text{SO}_4$  electrolyte in electrochemical cell specifically designed for meniscus method.<sup>7</sup> Sweep rate was 50 mV/s.



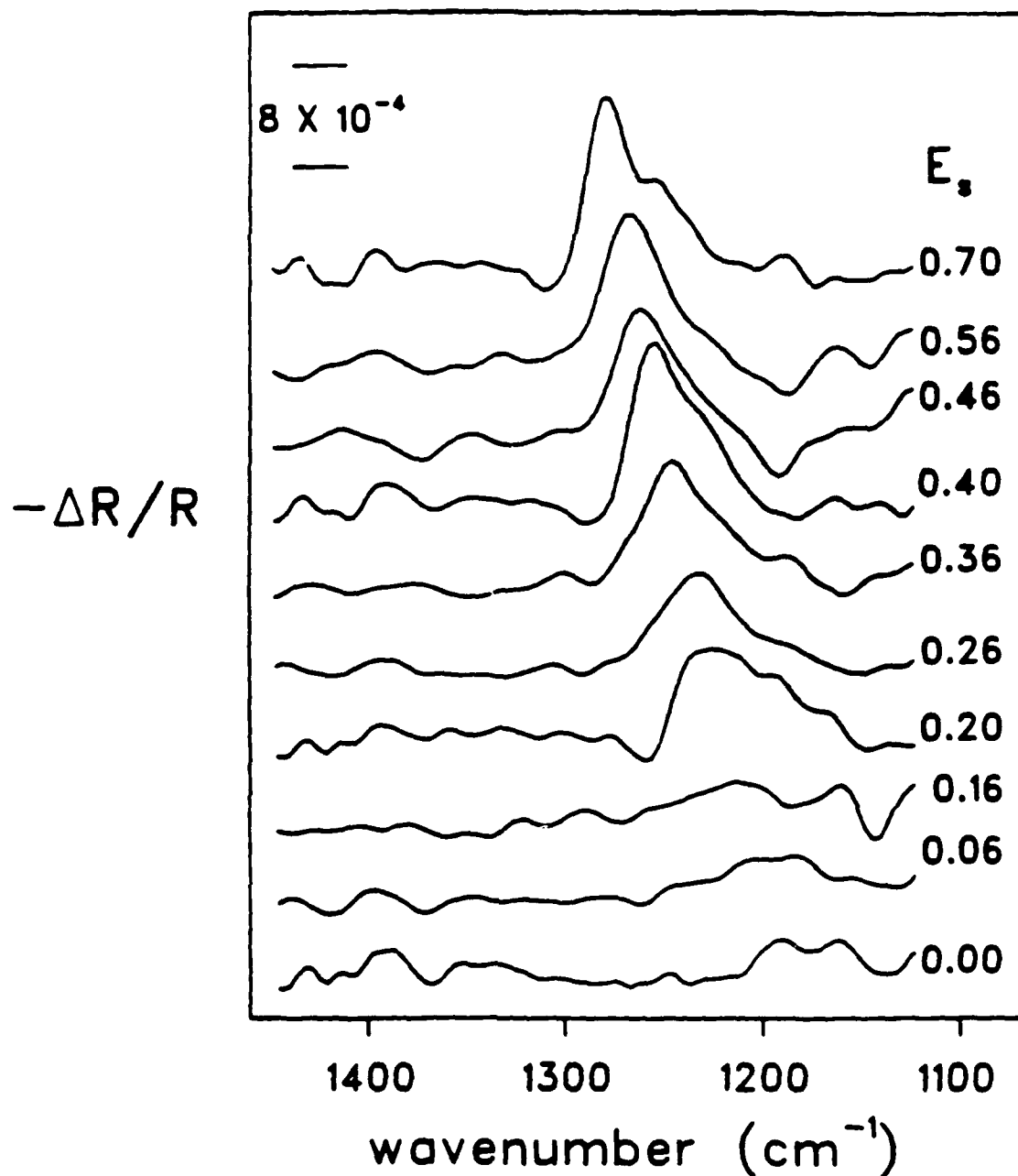


**Figure 4.** In situ FTIRRA spectra of Pt(111) single crystal electrode for 1450 - 1125  $\text{cm}^{-1}$ . Working electrode sample potentials  $E_s$  (V vs SCE) as noted in the figure. The reference potential,  $E_R = -0.26$  V. 8192 scans were co-added for each spectrum.



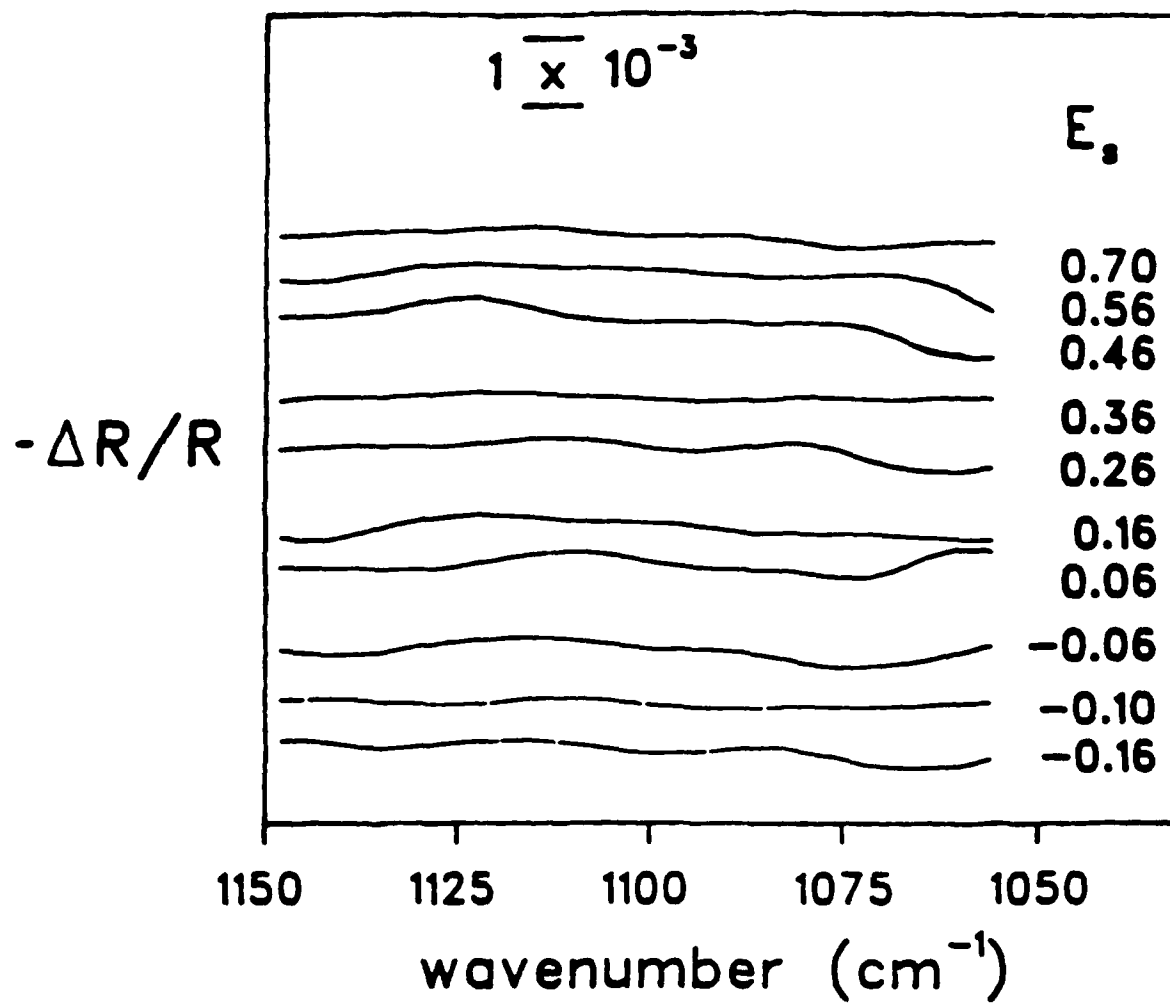


**Figure 5.** In situ FTIRRA spectra of Pt(111) single crystal electrode for 1150 - 1075  $\text{cm}^{-1}$ . Same conditions as in Figure 4.



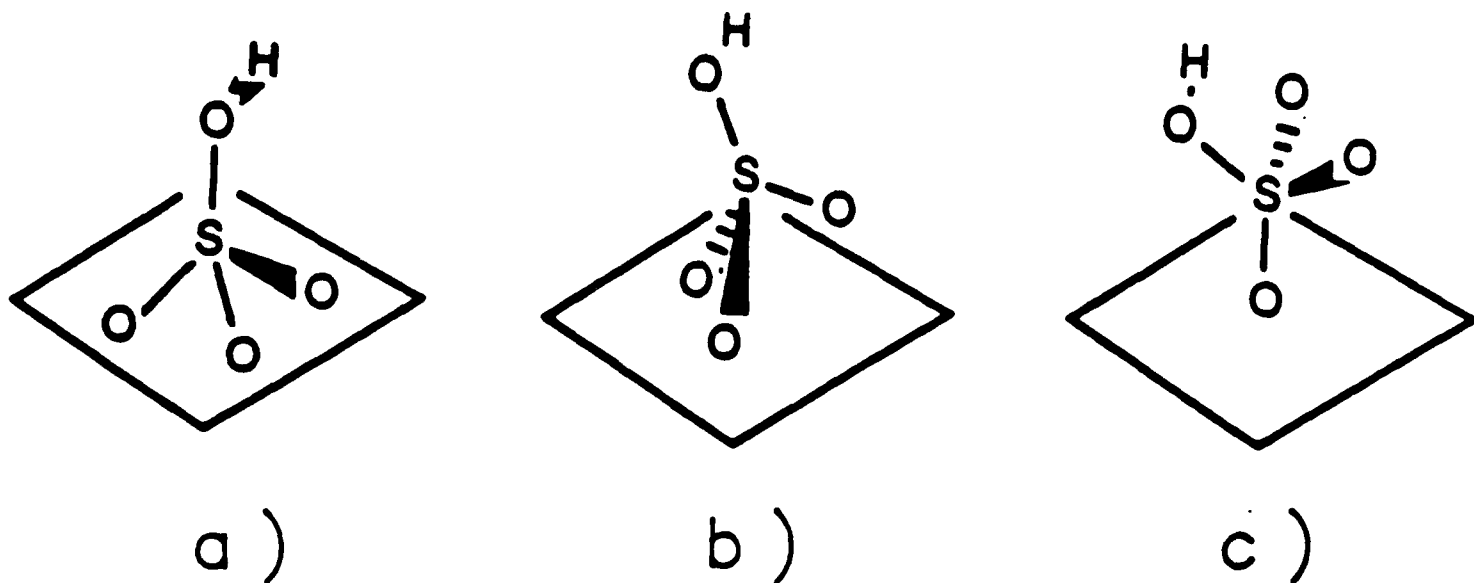


Figure 6. Schematic diagram of possible bisulfate adsorption orientation on an electrode surface: a) 3-fold interaction site, b) 2-fold interaction site, c) 1-fold interaction site.



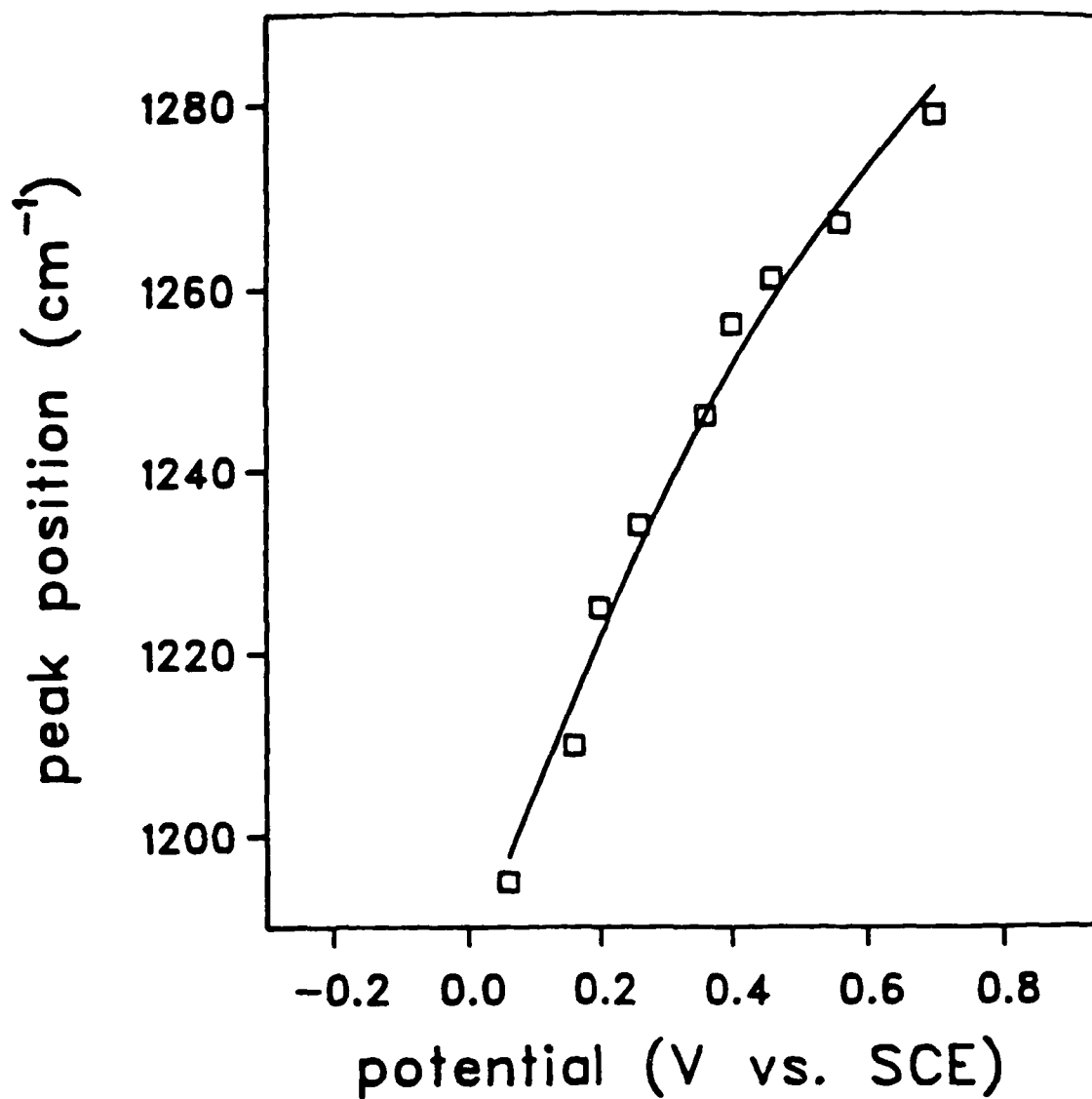
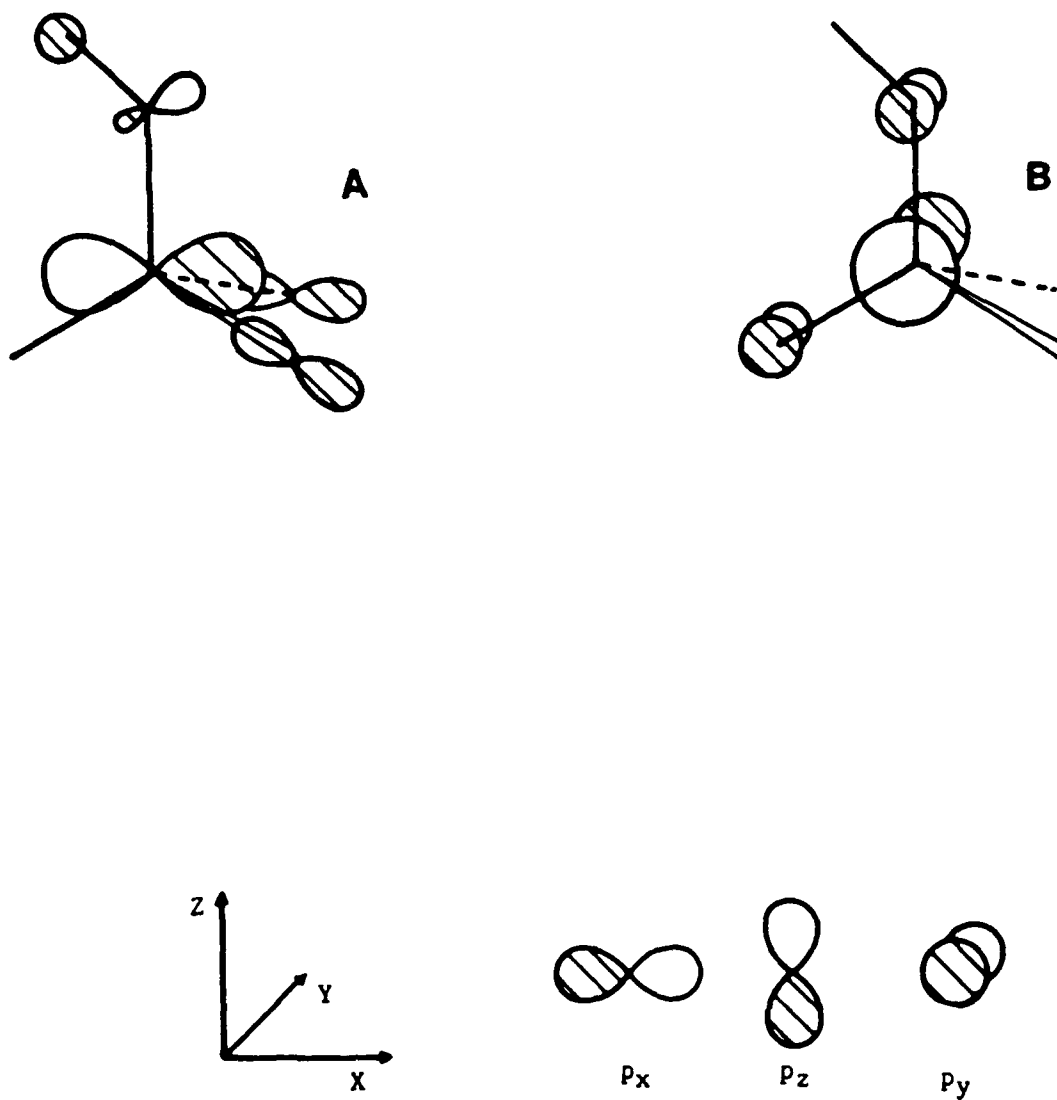


Figure 7. Potential dependence of bisulfate adsorption band peak maximum for Pt(111) single crystal electrodes in 0.05 M H<sub>2</sub>SO<sub>4</sub>.





**Figure 8.** Bisulfate molecular orbitals involved in adsorption on Pt(111): a)  $\sigma^*$  lowest unoccupied molecular orbital (LUMO), b)  $\pi^*$  LUMO. See text for details.



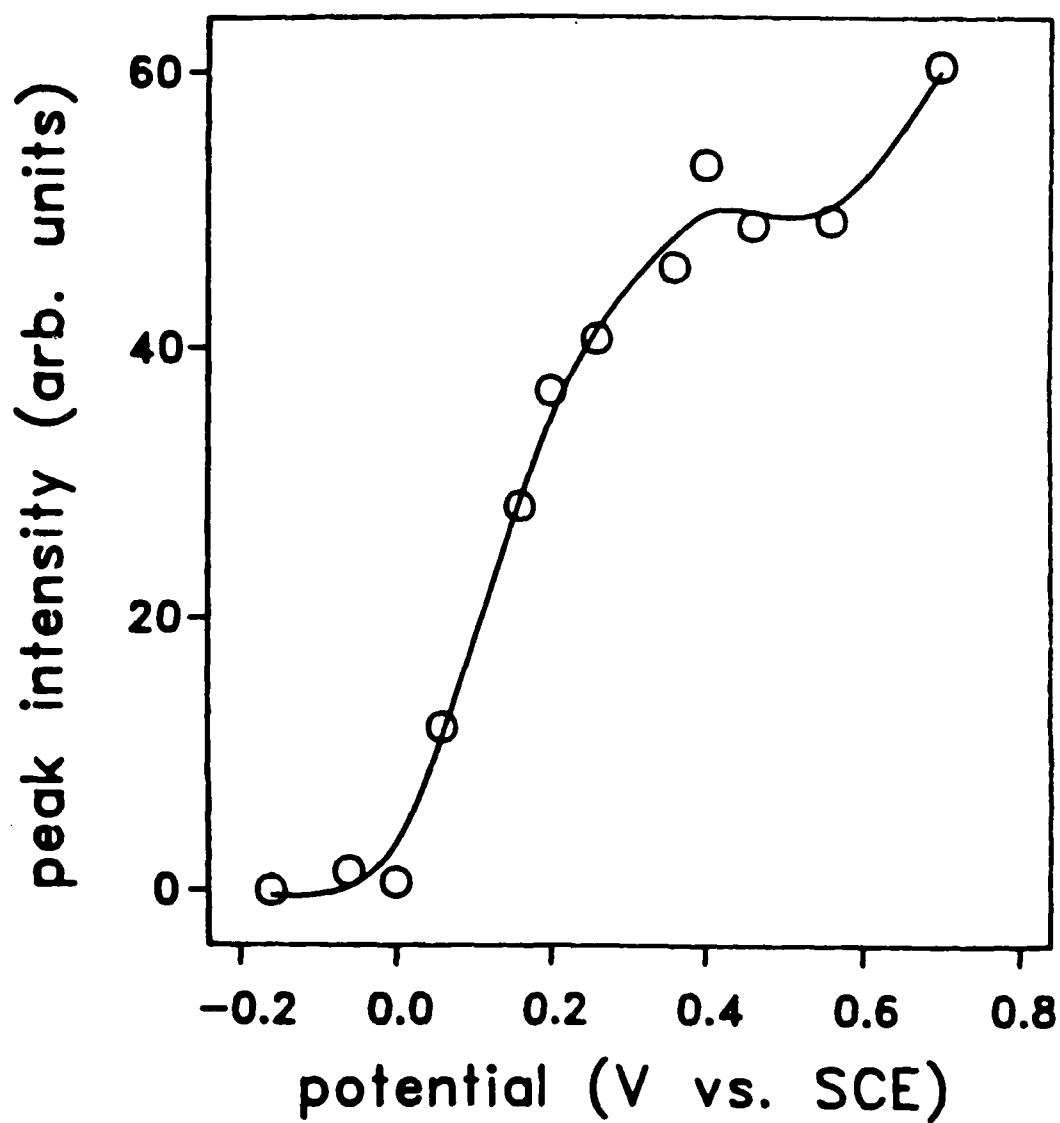
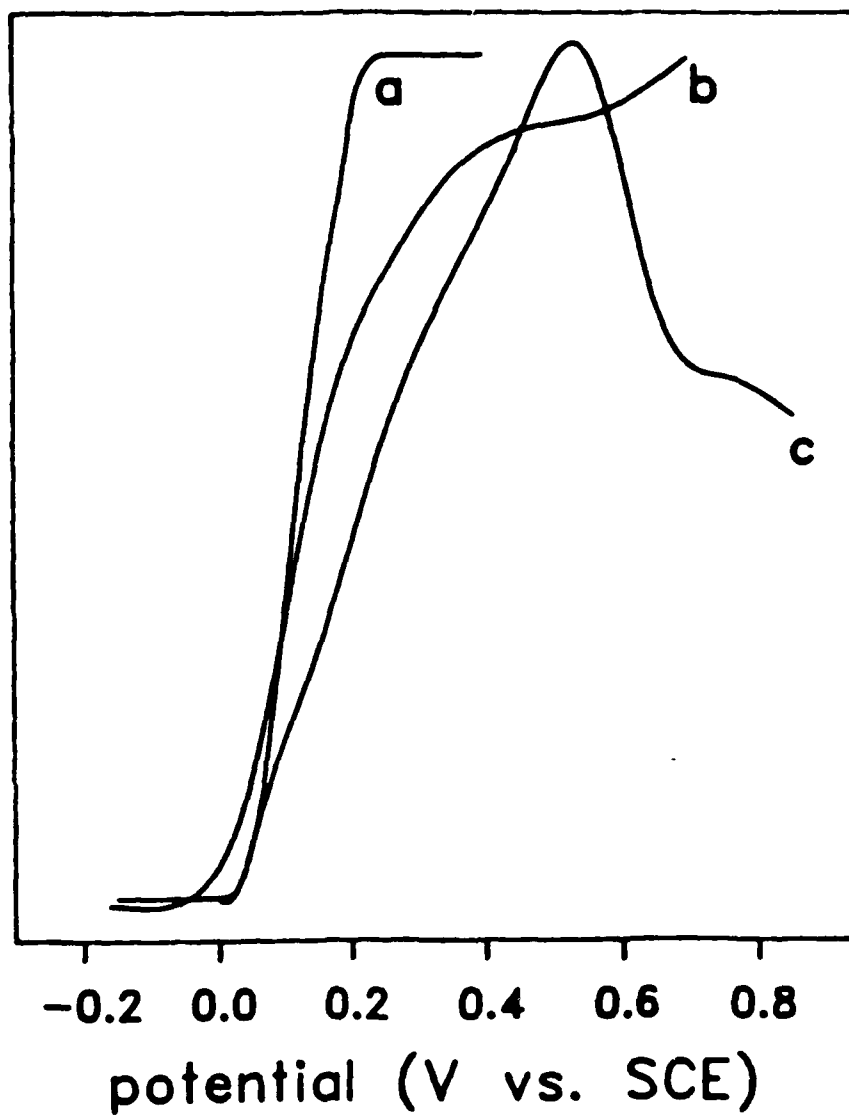


Figure 9. Potential dependence of corrected bisulfate adsorption integrated band intensity from spectra in Figure 4.





**Figure 10.** Potential dependence of a) normalized charge density, b) normalized band intensity (from Figure 9.) and c) normalized surface coverage of  $^{35}\text{S}$ -containing species (calculated from data taken from reference 6).



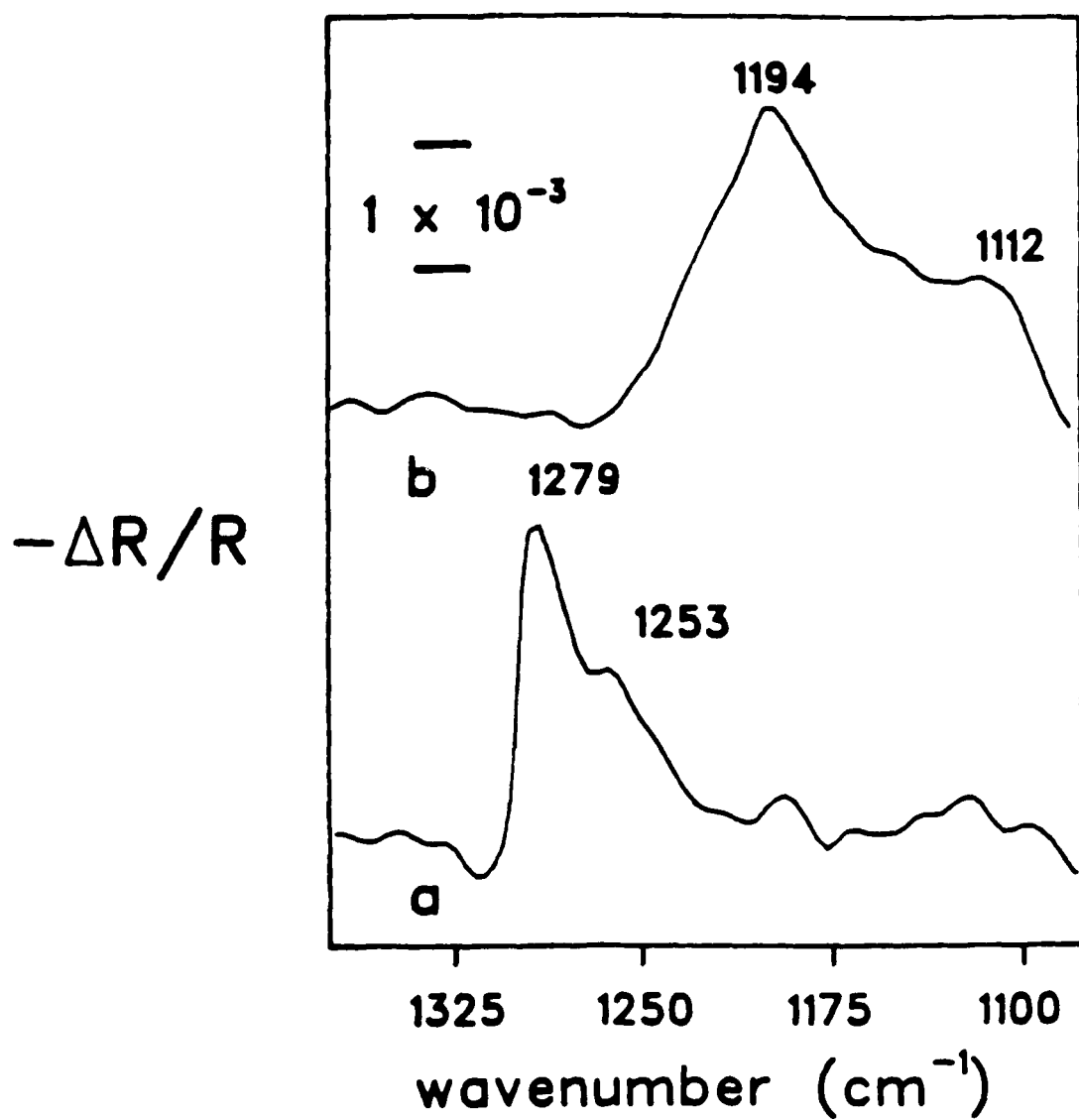


Figure 11. a) FTIRRA spectra same conditions as Figure 4,  $E_s = -0.7$  V. vs SCE. b) FTIRRA spectra same conditions as Figure 4,  $E_s = -0.9$  V.